Robust Sliding Mode Controller Design for the Line-of-Sight Stabilization

Moon-Sik Kim*, Jung-Joo Yun*, Gi-Sung Yoo* and Min-Cheol Lee**

* Department of Intelligent Mechanical Engineering, Pusan National University, Busan, Korea
(Tel : +82-051-510-3081; E-mail: k7m7s10@pusan.ac.kr, jjyoon@pusan.ac.kr, nedayks@chol.com)
**Department of Mechanical Engineering, Pusan National University, Busan, Korea
(Tel : +82-051-510-2439; E-mail: mclee@pusan.ac.kr)

Abstract: The line-of-sight (LOS) stabilization system is a precision electro-mechanical gimbals assembly for rejecting vibration to isolate the load from its environment and point toward the target in a desired direction. This paper describes the design of gimbals system to reject the disturbance and to improve stabilization. To generate movement commands for the actuators in the stabilization system, the control system uses a sensor of angular rotation. The controller is a DSP with transducer and actuator interfaces. Unknown parameters of the gimbals are estimated using the signal compression method. The cross-correlation coefficient between the impulse response from the assumed model and the one from model of the gimbals is used to obtain the better estimation. And SMCPE (sliding mode control with perturbation estimation) is used to control the gimbals. SMCPE provides robustness of the control against the modeling deficiencies and unknown disturbances. In order to compare the performance of SMCPE with the classical SMC, a sample test result is presented.

Keywords: line-of-sight stabilization, gimbals, DSP, signal compression method, sliding mode control with perturbation estimation

1. INTRODUCTION

The term of UAV (unmanned aerial vehicle) has been defined for all kind of unmanned aerial vehicle without regard to recovery, and control method since the late 1980s. A manned aerial vehicle is so dangerous such as taking a pilot's live in bad environment, however the UAV has no danger of it. Because of advantage of the UAV, it is used as a military reconnaissance plane in the militaries, and for acquiring an aerial image or observing a wide place in a civil field.

Especially for an unmanned helicopter, there are many advantages. For example, it has a little limitation of place when take-off and landing and it can take a photograph in a low altitude and stop state. However, it is difficult to acquire a high quality image because helicopter vibrates the camera mounted on it.

Therefore we develop the gimbals system for the line-of-sight stabilization system which can remove the vibration affected on the camera. The gimbals undergoes rotational motion about its center of rotation. In such an environment, the gimbals is mounted on a movable platform that is stabilized with respect to vehicle movement. When the vehicle undergoes rotational motion about its axes, the LOS remains fixed with respect to an inertial reference frame. This is accomplished by sensing these angular disturbances, and controlling the LOS system using the sensing values [1-2].

In this paper, we develop the digital-signal-processor (DSP) board to control the LOS system and apply the SMCPE algorithm to the LOS system. SMCPE is an enhanced version of the conventional SMC, which provides robustness of control against perturbation [3]. To apply this control algorithm, unknown parameters of the gimbals are estimated by using the signal compression method [4-5].

2. GIMBALS SYSTEM

2.1 Structure of gimbals

The mechanical design of gimbals is focused on coinciding axis of sight-of-camera mounted on the gimbals with axis of rotational motion of the gimbals. The accelerometers (ADXL202) mounted on the gimbals are used as tools to acquire angular information. They are used to get the angular disturbances of the two axes. Two DC motors are used to control the two axes (roll and pitch), and one RC motor is installed to control the one axis (yaw). This structure is assembled by gears, timing belt and linkage. Fig. 1 depicts the layout for the LOS stabilization system. Fig. 2 shows the picture for the developed gimbals system.

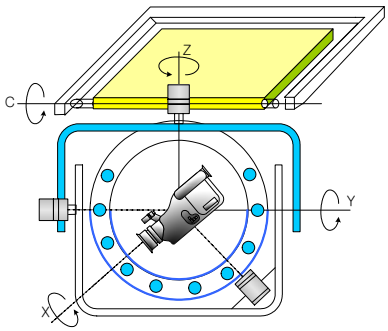

Fig. 1 Layout of the developed gimbals

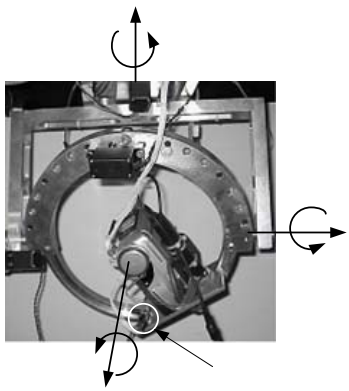

Fig. 2 Pictures of the developed gimbals

2.2 Sensing and motion control board

The gimbals controller is designed by using floating-point DSP (TMS320VC33-150) as shown in Fig 3. The DSP can perform a single-cycle floating-point operation every 13 nsec (150 MIPS) when 15MHz oscillator is used as external clock of PLL. 34k word of single-cycle program/data RAM are imbedded inherently.

The accelerometer (ADXL202) is used as 2-axes tilt sensor with faster response than electrolytic, mercury, or thermal sensors. The outputs are digital signals whose duty cycles (ratio of pulse width to period) are proportional to acceleration. The duty cycle outputs can be directly measured by a microprocessor counter without an A/D converter or glue logic. AVR-microprocessor (ATTINY26) is used as a 12 bit counter to counter the duty ratio of the sensor.

Two servo drivers are designed to activate two coreless DC motors. We develop DC motor drivers using N-TYPE FET and FET gate drivers. The drivers are operated by PWM input and some digital commands. Also, we use ATTINY26 as a PWM (1 KHz) generator and digital commander.

A serial communication chip (16C550) is on the board for the RS-232 communication between the DSP and PC. DSP transfers the information of the sensing values, some control values (sliding dynamics, torque, error et al.) to PC.

Fig. 3 illustrates the motion control board for gimbals system. Fig. 4 shows the picture of the control board.

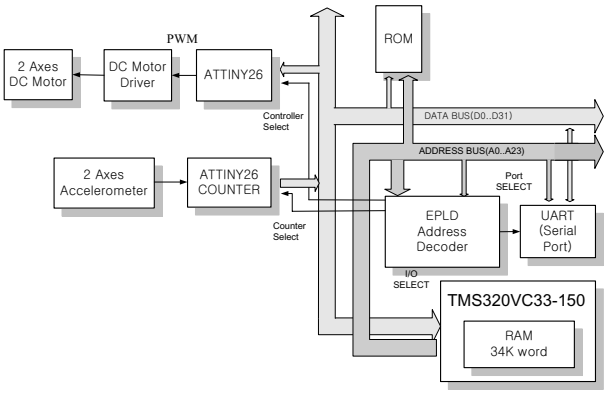

Fig. 3 Schematic diagram of the motion control board

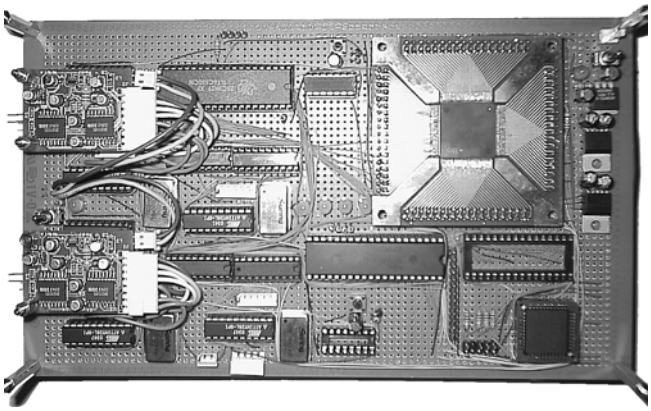

Fig. 4 Picture of the DSP motion control board

2.3 Identification of the gimbals

An ideal impulse has the flat power spectrum in a wide frequency range. However, it is sufficient in a practical measurement for an impulse to have a flat power spectrum in a limited frequency range. The waveform having such a property of impulse can be Fourier transformed and passed through a mathematical phase-shift filter. Then, the signal has a constant power and phase delay. If this signal in the frequency domain is transformed into the time domain through the inverse Fourier transformation, the test signal might have low amplitude and lasted for a long time. The test signal applied the each axis (roll and pitch) of the gimbals, in order to estimate uncertain parameters. A response obtained by supplying the system with the input signal can be compressed through fast Fourier transform (FFT), inverse phase-shift filter, and inverse fast Fourier transform (IFFT). These operations are all linear. Therefore, they can be interchangeable. This compressed signal is identical to an output signal when a pulse signal is supplied directly to the system. These processes as a whole are known as a signal compression method [4]. Fig. 5 shows the principle of the signal compression method. The bode plot of equivalent impulse response is compared with one of the impulse response of model which is same order as the gimbals. To compare bode plot, the cross-correlation coefficient is used. When the coefficient is maximum value, we can say that two responses are almost equivalent. In experiment, the proportion control strategy is used to prevent divergence of the response. Fig. 6 shows the block diagram of control scheme. The transfer function of the Fig. 6 is obtained as

$$G(s) = \frac{\theta(s)}{\theta_r(s)} = \frac{K_p K_m}{Js^2 + Bs + K_p K_m} = \frac{\omega_n^2}{s^2 + 2\zeta\omega_n s + K_p K_m} \qquad (1)$$

where K_m is constant of motor torque. Therefore, the relations of $J = \frac{K_p K_m}{\omega_n^2}$ and $B = 2\zeta\omega_n J$ are derived in Eq. (1). Fig. 7 and 8 show the power spectrum of the estimated second order system and result of experiment. Table 1 shows estimated parameters of the gimbals.

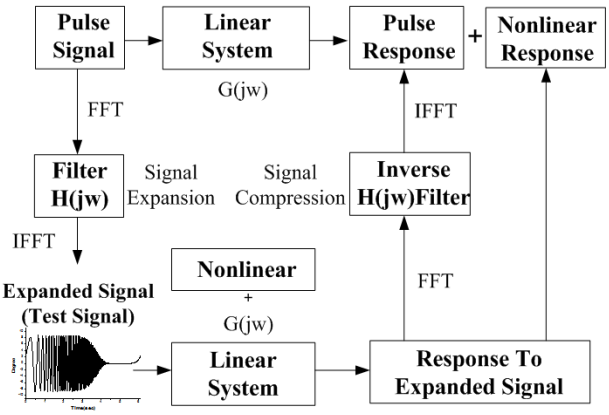

Fig. 5 Principle of the signal compression method

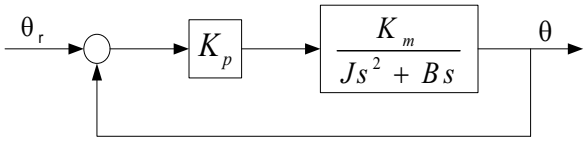

Fig. 6 Block diagram of the control scheme for signal compression method

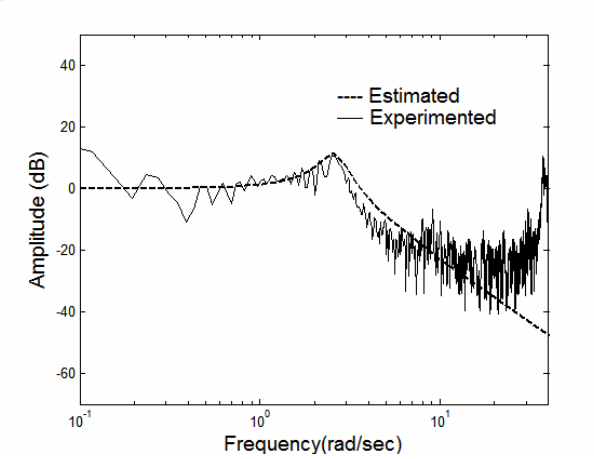

Fig. 7 Power spectrum of the roll motion

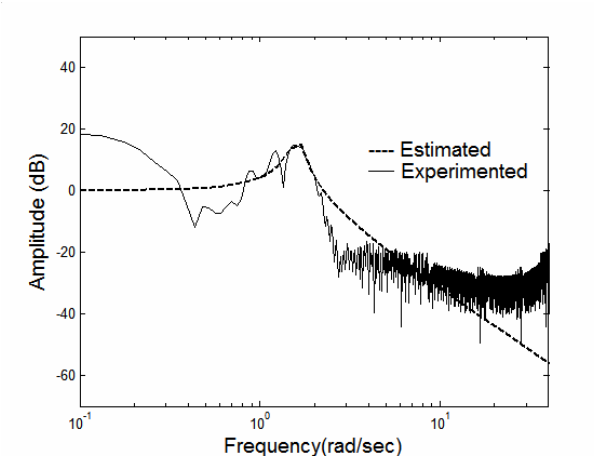

Fig. 8 Power spectrum of the pitch motion

Table 1 Estimated parameters of the gimbals

Parameters	Roll	Pitch
cross-correlation coefficient	0.924	0.857
$\omega_n(rad/\sec)$	3.7	3.1
ζ	0.17	0.18
K_p	1.5	0.5
K_m	5.53	5.53
$J(kg\cdot m^2)$	0.61	0.29
$B(kg\cdot m^2/s)$	0.77	0.32

3. SMCPE

3.1 Summary of perturbation estimation

The general representation of the nonlinear dynamics is defined as

$$\mathbf{x}^{(n)} = \mathbf{f(X)} + \mathbf{\Delta f(X)} + [\mathbf{B(X)} + \mathbf{\Delta B(X)}]\mathbf{u} + \mathbf{d}(t) \qquad (2)$$

where $\mathbf{X}_i = [x_i,\ \dot{x}_i, \cdots, x_i^{(n_i-1)}]^T \in$ ^{n_i} ($i = 1, \cdots, m$) is the state subvector, which is an element of the global state vector $\mathbf{X} = [\mathbf{X}_1^T, \mathbf{X}_2^T, \cdots, \mathbf{X}_m^T]^T \in$ ^{r}, $r = \sum_{i=1}^{m} n_i$, x_i ($i = 1, \cdots, m$) are m independent coordinates

$$\mathbf{x}^{(n)} = [x_1^{(n_1)}, x_2^{(n_2)}, \cdots, x_m^{(n_m)}]^T \in \quad ^{m},$$

$x_i^{(k)} \in$ is differential terms such as $x_i^{(k)} = \dfrac{d^k(x_i)}{dt^k}$, $\dot{x}_i = \dfrac{d(x_i)}{dt}$, and

$$\mathbf{f} = [\Delta f_1, \Delta f_2, \cdots, \Delta f_m]^T \in \quad ^{m},$$
$$\mathbf{\Delta f} = [\Delta f_1, \Delta f_2, \cdots, \Delta f_m]^T \in \quad ^{m}$$

are vector fields corresponding to the nonlinear driving terms and their perturbation.

$$\mathbf{B} = [b_{ij}] \in \quad ^{m\times m} \quad \text{and} \quad \mathbf{\Delta B} = [\Delta b_{ij}] \in \quad ^{m\times m} \quad (i, j = 1, \cdots, m)$$

are matrices representing the control gains and their uncertainties, respectively, $\mathbf{d} = [d_1, d_2, \cdots, d_m]^T \in$ ^{m} is the system disturbance vector, $\mathbf{u} = [u_1, u_2, \cdots, u_m]^T \in$ ^{m} is the control vector [3].

The perturbations $\mathbf{\Delta f}, \mathbf{\Delta B}$ and $\mathbf{d}$ are not known, neither are their upper bounds. $\mathbf{B} + \mathbf{\Delta B}$ is a square matrix and introduces coupling between the controls. We combine the perturbations in (2) is assumed as

$$\begin{aligned}\Psi(\mathbf{X},t)_{actual} &= \mathbf{\Delta f} + \mathbf{\Delta B u} + \mathbf{d} \\ &= \mathbf{x^{(n)}} - \mathbf{f} - \mathbf{B u} \quad .\end{aligned} \qquad (3)$$

If all components in the dynamics show slower variations with respect to the sampling speed, $\Psi(\mathbf{X},t)$ can be estimated as

$$\Psi(\mathbf{X},t)_{estimated} = \mathbf{x}_{calculated}^{(n)} - \mathbf{f} - \mathbf{B u}(t-\delta) \qquad (4)$$

where δ is the control sampling interval.

The estimation errors are caused by two sources. First, $\mathbf{x}^{(n-2)}$ measurements are often noisy. Especially, ADXL202's output is tilt information which is the value of $\mathbf{x}^{(n-2)}$. So we must differentiate the value two times. ADXL202's original noise characteristic is bad, so their calculated time derivatives may occur prohibitively large variations. The measurement noise of $\mathbf{x}^{(n-2)}$ must be filtered to a proper level. Second, because of one sample delay (δ), $u(t)$ is not equal to $u(t-\delta)$. In order to resolve the dilemma of causality, the current value of u is replaced by the most recent control $u(t-\delta)$. This replacement is difficult to justify stability when the control u manifests discontinuities as the switching function. Therefore, this discontinuity in control should be smoothened by using the saturation function.

Using the smoothened control $u \cong u(t-\delta)$ becomes a reasonable approximation. If the estimation errors are smaller than the actual perturbations, sliding mode control perturbation estimation (SMCPE) will outperform classical SMC. No matter how large the actual perturbations, the control strategy of SMCPE have the better the performance because of the smaller the perturbation estimation error [3].

3.2 Sliding mode control

The state space representation of general second order dynamics with m-degree-of-freedom sliding function is defined as

$$\mathbf{s} = \dot{\mathbf{e}} + \mathbf{c}_1 \mathbf{e} \tag{5}$$

where $\mathbf{s} = [s_1, s_2, \cdots, s_m]^T \in$ ^{m} : the sliding function,
$\dot{\mathbf{e}} = [\dot{e}_1, \dot{e}_2, \cdots, \dot{e}_m]^T \in$ ^{m}, $\dot{e}_j = \dot{x}_{1j} - \dot{x}_{1dj}$: the velocity tracking error,
$\mathbf{e} = [e_1, e_2, \cdots, e_m]^T \in$ ^{m}, $e_j = x_{1j} - x_{1dj}$: the position tracking error,
$[x_{1dj}\ \dot{x}_{1dj}] \in$ ^{2} : the desired trajectories of "j-th" degree of freedom,
$\mathbf{c_1} = diag(c_{1j})$, $c_{1j} > 0$: the slope of sliding function.

In order to satisfy the attractive condition (sliding mode condition: $\mathbf{s}^T\dot{\mathbf{s}} \le 0$) a desired $\mathbf{s}$ dynamics is selected as

$$\dot{\mathbf{s}} = \mathbf{-Ksat(s)} \tag{6}$$

where $\mathbf{K} = diag(K_j)$, $K_j > 0 \quad (j = 1, \cdots, m)$ and
$sat(s) = [sat(s_1), sat(s_2), \cdots, sat(s_m)]^T \in$ ^{m},

$$sat(s_j) = \begin{cases} s_j / |s_j|, & if\ |s_j| \ge \varepsilon_{sj} \\ s_j / \varepsilon_{sj}, & if\ |s_j| \le \varepsilon_{sj} \end{cases} \tag{7}$$

is used due to desirable anti-chattering properties. In expression (6), ε_{sj} stands for boundary layer of the SMC strategy.

We proposed the following control strategy

$$\mathbf{u = B^{-1}[-Ksat(s) - \alpha - f + x_d^{(n)} - \Psi(X,t)_{estimated}]} \tag{8}$$

where $\alpha_j = \sum_{k=1}^{n_j - 1} c_{j,k} e_j^{(k)}$. If we substitute (8) for $\mathbf{u}$ in (3), the relations are derived as

$$\begin{aligned} \mathbf{\Psi(X,t)_{actual}} &= \mathbf{x^{(n)} - f - [-Ksat(s) - \alpha - f + x_d^{(n)} - \Psi(X,t)_{estimated}]} \\ &= \mathbf{x^{(n)} - x_d{}^{(n)} + Ksat(s) + \Psi(X,t)_{estimated} + \alpha} \end{aligned}$$

$$\mathbf{\dot{s} = -Ksat(s) + \Psi(X,t)_{actual} - \Psi(X,t)_{estimated}} \ ,$$

$$\mathbf{\dot{s} + (\frac{K}{\varepsilon_s})s = \Psi(X,t)_{actual} - \Psi(X,t)_{estimated}} \ . \tag{9}$$

We assume that the influence of s terms in $\mathbf{\Psi(X,t)_{actual} - \Psi(X,t)_{estimated}}$ is negligible and dynamic response of s_j to this fluctuations is dictated by K_j / ε_{sj} matrix. Then low pass filter behavior of s_j is obtained by limiting its maximum break frequency to ω_{cj}

$$\omega_{cj} = K_j / \varepsilon_{sj} \ . \tag{10}$$

Fig. 9 shows the block diagram of SMCPE.

4. EXPERIMENT

4.1 Sensing problem

All experiments are executed at 200Hz as control loop

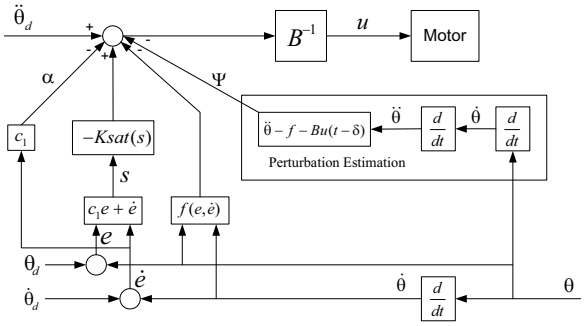

Fig. 9 Block diagram representation of SMCPE

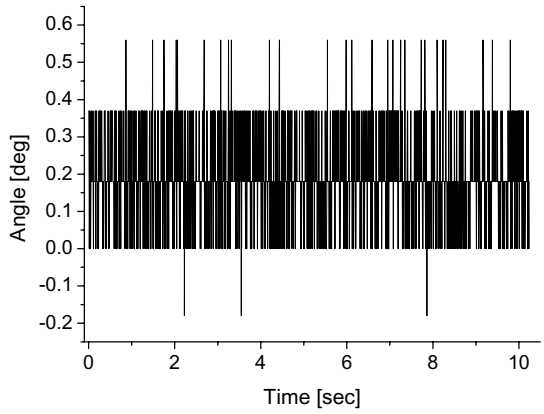

Fig. 10 Tilt sensor output in no actuating motor

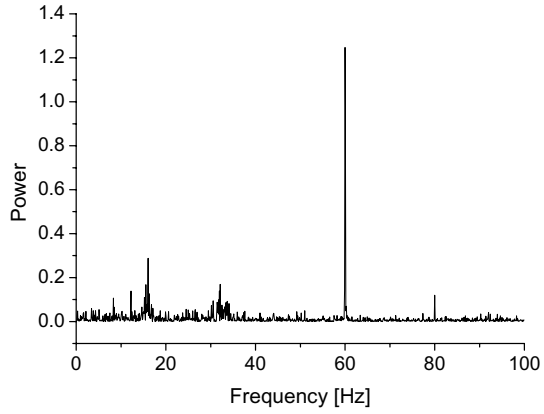

Fig. 11 Power spectrum of tilt sensor signal in no actuating motor

frequency. All control processes of sensing, SMC and PE are conducted in 5 msec. ADXL202's noise characteristic is not so good. Although dc motor doesn't work, the sensor has the chattering problem. Fig 10 and 11 show the sensor's noise characteristics.

Naturally, in actuating the motor, sensor signal has much more noise. In Fig. 10, noise signal has power in wide frequency range. Especially, it has maximum power at near of 60 Hz.

Because of sensor signal's noise characteristic, the

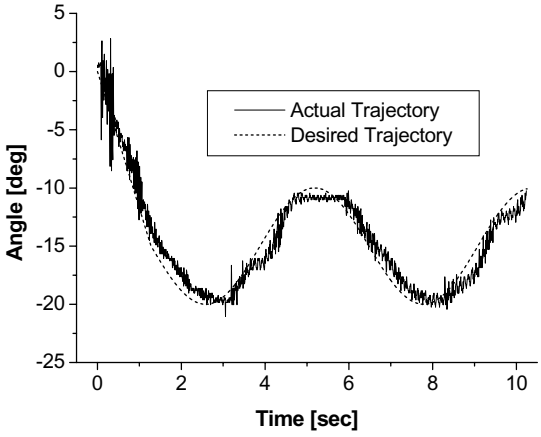

Fig. 12 Trajectories for SMC

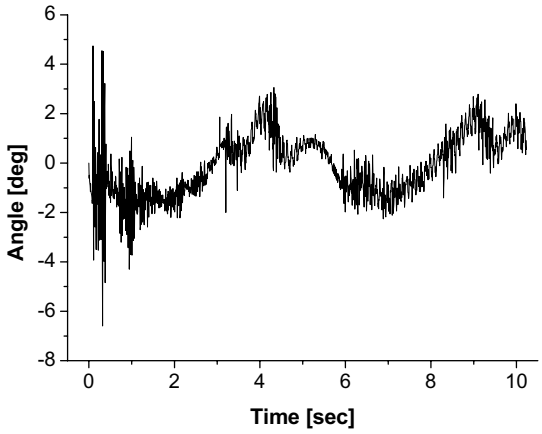

Fig. 13 Position tracking errors for SMC

differential value of sensor is added to noise terms. So we use the digital low pass filter for perturbation estimation.

4.2 Experiment result

The experiments are carried out in only roll. The performance of the SMC is compared with it of the SMCPE. We experiments the trajectory following control in place of absorbing the vibration and jitter because we have no vibrator or producer of jitter. All control parameters are experimentally determined.

The SMC control strategy is selected as

$$\mathbf{u = B^{-1}[-Ksat(s) - \alpha - f + x_d^{(n)}]} \tag{11}$$

and SMCPE's control strategy is expressed in (8).

Fig. 12 and 13 show the actual and desired trajectories, tracking errors for the SMC application. Tracking errors are almost within 2 degrees except for starting ranges (0~2 sec).

Fig. 14 and 15 also show tracking performances for the SMCPE application. The performance of the SMCPE is not superior to the SMC in tracking errors. So we compare the root mean square of tracking errors for the SMC with it for SMCPE.

The root mean square is

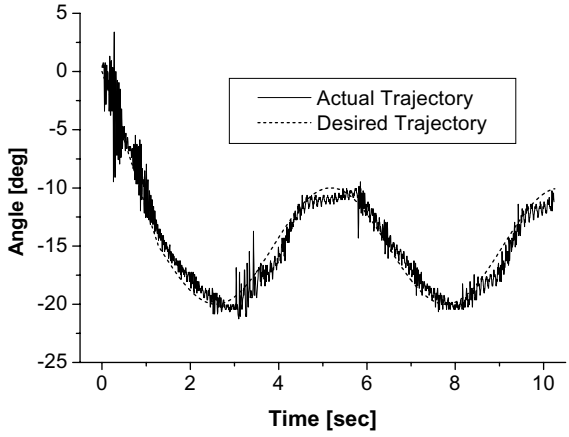

Fig. 14 Trajectories for SMCPE

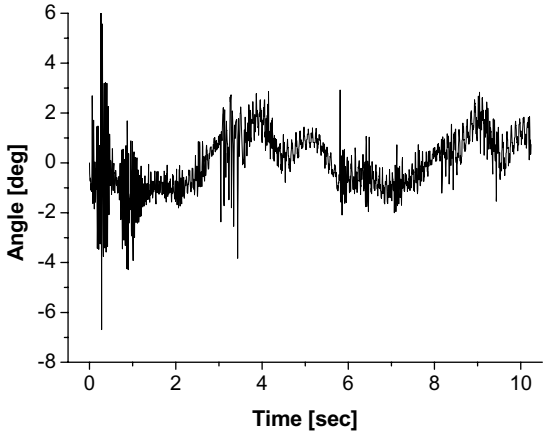

Fig. 15 Position tracking errors for SMCPE

$$e_{rms} = (\frac{1}{m}\sum_{n=1}^{m} e_n^{\,2})^{1/2} . \tag{12}$$

Using (12), the position tracking errors of the SMC are less than 1.24470° (RMS value) and the position tracking errors of SMCPE are within 1.14471° (RMS value). In root mean square of tracking errors, the errors of SMCPE have a decrease of 10% about compared with SMC. Therefore, it is shown that SMCPE strategy yields better performance with less control activity and is superior to the SMC strategy. The reason of this is caused by reducing noise in the velocity feedback and robustness against perturbations.

5. CONCLUSIONS

In this paper, we estimate the unknown parameters of gimbals with signal compression method. The parameter is used to estimate perturbation of the gimbals.

Generally, sliding mode control with perturbation estimation's performance is more excellent than conventional sliding mode control. But in this research, we use the sensor with terrible noise. For perturbation estimation algorithm, we use digital low pass filter. But it has the phase shift, and does

not cut off noise perfectly. Because differential value of sensor signal appears very large, performance of the perturbation estimation is not so good. It is observed that the tracking performance influences extremely the measurement noise.

In the further research, we will research about digital filters with no phase shift in operating range and robust sliding mode control algorithm in spite of sensor chattering.

ACKNOWLEDGMENTS

The authors would like to thank the Ministry of Science and Technology of Korea for financial support in the form of grant (M1-0203-00-0017-02J0000-00910) under the NRL (National Research Laboratory).

REFERENCES

[1] M. C. Algrain and J. Quinn, "Accelerometer based line-of-sight stabilization approach for pointing and tracking systems," *Second IEEE Conf. on Control Application*, Vol.1, pp. 159 – 163, 1993.

[2] Y. S. Kang, "Friction identification of a sight stabilization system and feasibility study on its application to control performance improvement," Ph. D dissertation KAIS, KOREA, 1997.

[3] H. Elmali and N. Olgac, "Implementation of sliding mode control with perturbation estimation(SMCPE)," *IEEE Trans. on Control System*, Vol. 4, No. 1, pp. 79-85, 1996.

[4] M. K. Park and M. C. Lee, "Identification of a hydraulic simulator using the modified signal compression method and application to control," *IEEE Trans. On Automatic Control,* Vol. pp. 1111-, 2000.

[5] N. Aoshima, "Microprocessor-Based system identification by signal compression method," D. Reidel Pub. Com. , pp. 81-103, 1986.